Anatomy Based 3D Dose Optimization in Brachytherapy Using Multiobjective Genetic Algorithms

M. Lahanas
Department of Medical Physics & Engineering, Strahlenklinik, Städtische Kliniken Offenbach, 63069 Offenbach, Germany.

D. Baltas and N. Zamboglou
Department of Medical Physics & Engineering, Strahlenklinik, Städtische Kliniken Offenbach, 63069 Offenbach, Germany.
and
Institute of Communication & Computer Systems, National Technical University of Athens, 15773 Zografou, Athens, Greece.

Corresponding author:
Dimos Baltas, Ph.D.
Dept. Of Medical Physics & Engineering
Strahlenklink
Städtische Kliniken Offenbach
Starkenburgring 66
63069 Offenbach am Main, Germany
Tel.: +49 – 69 – 8405 –4480 or –3335 (Secretary)
Fax. : +49 – 69 – 8405 –4481 or –864480
E-mail: dbaltas@compuserve.com

Abstract

In conventional dose optimization algorithms, in brachytherapy, multiple objectives are expressed in terms of an aggregating function which combines individual objective values into a single utility value, making the problem single objective, prior to optimization. A Multiobjective Genetic Algorithm (MOGA) was developed for dose optimization based on *a posteriori* approach, leaving the decision making process to a planner and offering a representative trade-off surface of the various objectives. The MOGA provides a flexible search engine which provides the maximum of information for a decision maker. Tests performed with various treatment plans in brachytherapy have shown that MOGA gives solutions which are superior to those of traditional dose optimization algorithms. Objectives were proposed in terms of the COIN distribution and differential volume histograms, taking into account patient anatomy in the optimization process.

Key words: Optimization, Brachytherapy, COIN, Dose-volume histograms, Multiobjective genetic algorithms.

Introduction

We consider the problem of the optimization of the three dimensional dose distribution in HDR brachytherapy using a single stepping source. Given n possible source positions (dwell positions) the problem is the determination of n weights (dwell weights) or times (dwell times) so that the resulting dose distribution will fulfill defined quality criteria. In modern brachytherapy, as distinct from classical brachytherapy, the dose distribution has to be evaluated with reference to the planning target volume (PTV) and irradiated normal tissues[1,2,3,4,5]. Recently, a dose-volume histogram based method called Conformal Index (COIN)[6] has been proposed to evaluate the quality of 3D brachytherapy dose distributions. The aim of optimization is to produce a dose distribution which matches the clinical goals which are to achieve a homogeneous dose value on the surface of the PTV, to limit areas of very high dose values within the PTV and to achieve an extremely rapid fall-off of dose outside the PTV. Additionally, critical structures maybe within or adjacent to the PTV. In this situation the dose must be smaller than a critical dose value D_{crit}. In practice, it is difficult if not impossible to meet all these objectives simultaneously. In the past some efforts have been made with algorithms developed which try to achieve some of the previously mentioned criteria using phenomenological methods [7,8,9]. Most of these algorithms only take into account the catheter geometry and ignore the geometry of the PTV and critical structures. Some methods use points on the surface on the PTV and try to optimize the dose distribution by requiring that the isodose surface should ideally conform to the shape of the PTV. An additional term simultaneously added to the optimization function is used to minimize the inhomogeneity of the dose distribution within the PTV[7,9]. The final optimization function is then built as the weighted sum of both terms. The weights used are a measure of the significance of each term in the optimization process. Doses in adjacent critical structures are minimized, by trial and error, by manually changing the dwell times of dwell positions in the neighborhood of the critical structures.

Recently methods have been published[10,11] for brachytherapy dose distribution optimization of permanent implants in the prostate. Although these consider the dose distribution in anatomical regions such as the PTV and critical structures as urethra, they use similar cost functions consisting of a weighted sum of several objectives. For the minimization of the cost function they use a genetic single objective algorithm. Both published methods[10,11] are valid for permanent implants, where in contrast to the single stepping source technique, the dwell time has a binary form 0 or 1.

The use of a single weighted sum leads to information loss and is not generally to be recommended, especially for the case where objectives have not the same dimensions and in addition maybe competing. An understanding of which objectives are competing or non-competing is valuable information. The optimization problem in external beam radiotherapy and also in brachytherapy is exactly relevant to the application of multiobjective optimization methods where the maximum information is available.

In this paper, we present a multiobjective genetic algorithm (MOGA) for dose optimization in brachytherapy using a single HDR stepping source, based on the varying of dwell times (weights) where the dwell positions of the source are fixed. The entire anatomical information is taken into account by using dose-volume histograms (DVHs) for the PTV and for normal tissues and their evaluation according to the COIN distribution. The main characteristics of the new algorithm are described and its application in some clinical implants as well as in some test implants are demonstrated.

Multiobjective Optimization

Introduction and Definitions

The multiobjective optimization (*MO)* problem (also called multicriteria optimization or vector optimization) can be defined as the problem of determining[12]:

> "A vector of decision variables which satisfies constraints and optimizes a vector function whose elements represent the objective functions. These functions form a mathematical description of performance criteria which are usually in conflict with each other. Hence, the term optimize means finding such a solution which would give the values of all objective functions acceptable to the designer."

We call decision variables x_j, j=1,2,...,n for which values are to be chosen in an optimization problem. In order to know how "good" a certain solution is, we need to have some criteria for evaluation. These criteria are expressed as computable functions $f_1(\mathbf{x}),..., f_k(\mathbf{x})$ of the decision variables, that are called *objective functions*. These form a vector function **f**. In general, some of these will be in conflict with others, and some will have to be minimized while others are maximized.

The multiobjective optimization problem can be now defined as follows:

Find the vector $\mathbf{x}=(x_1,x_2,...,x_n)$ which will satisfy the m inequalities:

$g_i(\mathbf{x})>0, i=1,2,...,m$

the p equality constraints:

$h_i(\mathbf{x})=0, i=1,2,...,p$

and optimize the vector function **f**.

The constraints define the feasible region **X** and any point **x** in **X** defines a feasible solution. The vector function **f**(**x**) is a function which maps the set **X** in the set **F** which represents all possible values of the objective functions. Certain types of constraints such as bounds can be handled by mapping the search space so as to minimize the number of unfeasible solutions. Normally we never have a situation, like this, in which all the $f_i(\mathbf{x})$ values have a minimum in **X** at a common point **x**. We have to establish certain criteria to determine what would be considered an "optimal" solution. One interpretation of the term optimum in multiobjective optimization is the Pareto Optimum, formulated by Vilfredo Pareto in 1896. For two vectors $\mathbf{x}=(x_1,x_2,...,x_n)$ and $\mathbf{y}=(y_1,y_2,...,y_n)$ of the same dimension, *equality* and *less than* and *greater than* relationships are fulfilled if the relationships are true element by element. A fourth *partial less than* relationship can be defined as follows:

x is partially less than **y** if $\forall\, i \in \{1,...,n\}: x_i \le y_i \wedge \exists\, i \in \{1,...,n\} \mid x_i < y_i$. For minimization problems if **x** is partially less than **y** it is said that **y** is *dominated* by **x** or **y** is *inferior* to **x**.

We say that a point $\mathbf{x}^*$ in **X** is *Pareto optimal* if and only if there is no $\mathbf{x} \in \mathbf{X}$ for which **f**(**x**) dominates $\mathbf{f}(\mathbf{x}^*)$, i.e., there is no **x** such that for k objectives:

$$\forall\, i \in \{1,...,k\},\ f_i(\mathbf{x}) \le f_i(\mathbf{x}^*) \quad \wedge\ \exists\ i \in \{1,...,k\} \mid f_i(\mathbf{x}) < f_i(\mathbf{x}^*)$$

Each element in the Pareto-optimal set constitutes a non-inferior solution to the MO problem.

The problem has usually no unique, perfect solution, but a set of equally efficient, or non-inferior, alternative solutions, known as the **Pareto-optimal** set. Each point in this set is optimal in the sense that no improvement can be achieved in one vector component that does not lead to a degradation in at least one of the remaining components. That is, there are no other solutions superior in all attributes. The set of non-dominated solutions lie on a surface known as the *Pareto optimal frontier*.

In most cases, there will be several optimal solutions in the Pareto sense, and we have to look to the values of the objective functions in order to decide which values seems the most appropriate. This process in which a solution is selected is called the *decision making* process.

Optimization Strategies

Depending on how the computation and the decision processes are combined in the search for compromise solutions, three classes of MO methods exist according to Fonseca et al.[13,14]:

- ***A priori* method**: The decision maker expresses preferences in terms of an aggregating function which combines individual objective values into a single utility value, and ultimately makes the problem single objective, prior to optimization. The decision maker is required to produce a priority ranking of the objectives. Then some optimization engine steered by the formulation of the objectives and the priority ranking presents if possible a single global solution.
- **A p*osteriori* method**: The decision maker is presented by the search engine with a set of candidate non-inferior solutions, before expressing any preferences. The compromise solution is chosen from that set. The goal of the a *posteriori* method is to find and maintain a representative sampling of solutions on the Pareto frontier. The decision maker then selects the solution from the Pareto optimal set. The *a posteriori* method has the advantage that the results are independent of any decision making process and it is of greater use than in the a *priori* method since all possible solutions are represented by the Pareto frontier.
- **Progressive articulation of preferences method**: Decision making and optimization occur at interleaved steps. At each step, partial preference information is supplied by the decision maker to the search engine, which, in turn, generates better alternatives according to the information received. Interactively refining preferences have the potential advantage of reducing computational effort by concentrating optimization effort on the region from which compromise solutions are more likely to emerge, while simultaneously providing the decision maker with information on which preference refinement can be based.

Problems encountered with the use of weighted sums in optimization procedures

We consider now the conventional dose optimization algorithms where multiple objectives are expressed in terms of an aggregating function by combining the individual objectives values into a single utility value, making the problem single objective, prior to optimization, see for example the work of Yang et al.[11]. For two objectives f_1 and f_2 the aggregating function (or *cost function*) is:

$$w_1 \cdot f_1(\mathbf{x}) + w_2 \cdot f_2(\mathbf{x}) \qquad (1)$$

where w_1 and w_2 are weights so that $w_1+w_2=1$. The weights w_1 and w_2 express the importance of each term in the optimization process. We assume that for a given combination of weights the optimization result is the point 1 in Fig. 1a, which shows the set **F** (*bi-loss map)* in the objective space. The boundary of this set from A to B is the Pareto optimal frontier. Point 1 would be acceptable for the objective f_1, but probably not for f_2. Point 2 we could obtain by another set of weights but it could be unacceptable for f_2. An ideal solution could be point 3 but it is not known which combination of weights we must use to obtain this point in **F** after the optimization of Eq. 1.

One method which we could use to obtain points on the Pareto frontier would be to use a reasonably large number of combinations for w_1 and w_2. For each such combination, where $w_1+w_2=1$ we obtain a point on the Pareto frontier.

Even if we use a evenly distributed set of weights it is possible that the points which we obtain on the Pareto frontier are not uniformly distributed as shown in Fig. 1b. If the Pareto frontier is non-convex (Fig. 1c) then parts of the Pareto frontier become inaccessible due to minimizing any convex combination of the two objectives (e.g. point 1 in Fig 1c). If there exists a solution $\mathbf{x}^* \in \mathbf{F}$ (so called *utopia point* or *shadow minimum*) that simultaneously

succeeds in optimizing each objective, then the weighted sum can be reasonably satisfactory because then the optimization is expected to optimize each objective f_i.

For a given weight combination we obtain only a single point on the Pareto optimal frontier which is the set of all possible optima for multiobjective problems. The generation of points by minimizing weighted sums of objectives is limited to convex sets and usually produces a non-uniform distribution of points. Methods such as the Normal-Boundary Intersection Method[15] (NBI) exist which produce an even spread of points on the Pareto frontier but are limited for those cases where the objectives can be expressed as analytic functions of the decision variables. This is for example not the case where dose-volume histogram based objectives are used. This will be discussed later in more detail.

METHODS

A. Genetic Algorithms

By maintaining a population of solutions, genetic algorithms (GA) can search for many non-inferior solutions in parallel. This characteristic makes GAs very attractive for solving MO problems.
A genetic algorithm is according to Koza[16]:

> ''A highly parallel mathematical algorithm that transforms a set (population) of individual mathematical objects (typically fixed-length character strings patterned after chromosome strings), each with an associated fitness value, into a new population (i.e., the next generation) using operations patterned after the Darwinian principle of reproduction and survival of the fittest and after naturally occurring genetic operations (notably sexual recombination)''

Usually a genetic algorithm has the following components[17]:

- A representation of potential solutions to the problem
- A method to create an initial population of potential solutions
- An evaluation function that plays the role of the environment, rating solutions in term of their fitness.
- Genetic operators that alter the composition of the population members of the next generation.
- Values of various parameters that the genetic algorithm uses (population size, probabilities of applying genetic operators, etc.)

Genetic algorithms have a significant advantage over other search systems because instead of using a single searcher, as in calculus based search methods, a population is used making GA less probable to be trapped by local extremes.

Optimizations with GA are not limited to non-continuous or unimodal functions and therefore a larger class of problems can be solved than with traditional, gradient based search methods.

Problems in Multiobjective Optimization

In multiobjective optimization although populations are able to search many local optima, a finite population tends to settle on a single good optimum, even if other equivalent optima exist. This phenomenon is known as *genetic drift*. Niche induction methods promote the simultaneous sampling of several different optima by favouring diversity in the population. In order to simulate individual competition for finite resources in a geographical environment, fitness sharing models can be used. Individuals close to one another mutually decrease each other's fitness. Even if initially considered less fit, isolated individuals are thus given a greater change of reproducing, favouring diversification. In order to prevent the population forming niches (crowds) and since we want to have a uniform distribution over the Pareto frontier sharing to the population can be applied based on the niche count n_i of each member. The *niche count* n_i is an estimate of the number of individuals in the neighborhood of the i^{th} member[18].

$$n_i = \sum_{j=1}^{n} Sh[d[i,j]] \qquad (2)$$

$$Sh[d[i,j] = \begin{cases} 1 - \dfrac{d[i,j]}{s_{share}} & \text{if } d[i,j] < s_{share} \\ 0 & \text{else} \end{cases} \qquad (3)$$

σ_{share} is the sharing radius, d[i,j] is the Euclidean distance of the objectives of the individuals i and j. An estimation of the sharing radius for n objectives is:

$$s_{share} = \left(\frac{\text{Pareto Area}}{\text{Population size}} \right)^{\frac{1}{n-1}} \qquad (4)$$

Assuming that we know, or can estimate, the extreme situations of best and worst for each objective then the minimum size of the Pareto frontier (Pareto area) for two objectives f_1 and f_2 is simply the length:
and for the maximum size of the Pareto frontier we have:
In its basic form a population evolves into the next generation with proportional replication, which reproduces a member with a probability proportional to its fitness. Crossover and mutation are then performed on the members of this population. The proportional replication

$$\min(\text{Pareto area}) = ((f_1^{best} - f_1^{worst})^2 + (f_2^{best} - f_2^{worst})^2)^{\frac{1}{2}} \qquad (5)$$

in multiobjective optimization has to be modified, since for every member of the population a

$$\max(\text{Pareto area}) = \left| f_1^{best} - f_1^{worst} \right| + \left| f_2^{best} - f_2^{worst} \right| \qquad (6)$$

vector of fitness values is assigned with components for the value of each objective function. Three major different replication procedures are known with multiobjective optimization.

Nondominated Ranking Genetic Algorithm (NRGA)

Fonseca and Fleming[13] have proposed a selection method based on the rank of each member. For an individual at generation t with the corresponding objective vector **x** a rank is assigned given by:

$$rank(\mathbf{x},t)=1+n_{\mathbf{x}}^{t} \qquad (7)$$

where $n_{\mathbf{x}}^{t}$ is the number of individuals in the current population which are preferable to it. All non-dominated individuals are assigned rank 1, while dominated individuals are penalized according to the population density of the corresponding region of the trade-off surface (niche count). Fitness assignment is performed in the following way:

- The population is sorted according to rank.

- Fitness for individuals is assigned by interpolating from the best (rank 1) to the worst (rank n) in the way proposed by Goldberg[19], according to some function, such as:

Niched Pareto Genetic Algorithm (NPGA)

Horn and Nafpliotis[20] proposed a tournament selection scheme based on Pareto dominance. Instead of limiting the comparison to two individuals, a number of other individuals in the

$$\frac{\text{Population size}}{\text{rank}(x,t)} \qquad (8)$$

population were used to help determine dominance. When both competitors were either dominated or non-dominated (i.e., there was a tie), the result of the tournament was decided through fitness sharing. Population sizes considerably larger than usual were required so that the noise of the selection method could be tolerated by the emerging niches in the population.

The pseudocode for Pareto domination tournaments proposed by Horn and Nafpliotis is given below:

Take two random members m_1, m_2
From the remaining individuals take d random members
Call this set S
if m_1 is dominated by the set S
and m_2 is not dominated by S
select m_2
else
if m_2 is dominated by the set S
and m_1 is not dominated by S
select m_1
else
if neither or both are dominated by S
Select from the set of m_1 and m_2
member with the smallest niche count.

Non-Dominated Sorting Genetic Algorithm (NSGA)

Srinivas and Deb[21] proposed a method to classify individuals in layers, before the selection is performed. All non-dominated individuals are classified into one category with a dummy fitness value shared in order to maintain a diversity. These classified individuals are ignored and from the remaining members of the population the non-dominated are selected for forming the next layer. This process continues until all members are classified. Individual of the first layer have the highest fitness while to members of the last layer the smallest fitness is assigned. Individuals from the first layer produce more copies in the next generation therefore the population converges towards the Pareto frontier. Fig. 2 shows the flowchart of the NSGA selection method.

Optimization Variables

Each chromosome string consists of n dwell weights from 0 to 1. Two representations are used:

1) as an array of n double precision variables.
2) encoded as binary strings. The number of bits per dwell weight can be selected by the accuracy which is required.

We use as default 15 bits per dwell weight.

$$COIN = c_1 \cdot c_2 \qquad (9)$$

It should be noticed that our optimization variables are relative weights. In contrast to previous single objective genetic algorithms developed for permanent implants[11] where the weights are of binary type taking the value 0 or 1 and for this case the search space is limited to 2^n configurations for n weights, our search space for the double precision encoding has 2^{64n} configurations.

One additional advantage is that the NPGA and NRGA algorithms use a selection method which is not based on the fitness value, which is often an arbitrary value. The genetic algorithms of Yu et al.[10] and Yang et al.[11] use a weighted sum to be minimized. Since usually the selection methods of single objective genetic algorithms are based on the concept of the fitness of members of the population, which must be maximized in the optimization process, a fitness function is proposed which is equal to the inverse of the weighted sum. Our genetic algorithm uses a selection method which is based not on arbitrary sums and weights but on the concept of dominance.

B. Brachytherapy Dose Distribution Optimization Procedure

In contrast to the well established criteria for optimization of the 3D dose distribution in external beam radiotherapy[22], there are not common accepted criteria for the optimization of brachytherapy dose distributions. The main difference is that in case of brachytherapy there will be always a high inhomogeneity of the dose distribution near the sources where high dose gradients exist. In general, optimization of the dose distribution in brachytherapy means established quality criteria have to be satisfied and that the corresponding parameters describing the quality of the distribution have to be maximized. For the case of the anatomyless evaluation of the dose distribution criteria used are related to uniformity indexes and indexes describing volumes with high dose values[1,6]. In addition optimization techniques are focused to reduce the variance of dose values on so called *dose points* defined geometrically and thought to represent some anatomical structures like PTV. Optimization means to maximize the quality of the dose distribution. The problem is how to quantitatively define the term of quality. Several parameters have been proposed to describe the quality of a brachytherapy application[6]. Most of them are based only on the dosimetric characteristics without considering the patient anatomy. The Conformal Index COIN allows the expression of the quality of a given dose distribution according to its conformity relative to the PTV and critical structures. It is based on the dose-volume histograms calculated for all relevant type of tissues. A real optimization strategy has to consider the quality of the brachytherapy dose distribution in relation to PTV and organs at risk. COIN can be used as a quality index for the optimization procedure.

The Conformal Index (COIN)

In Baltas et al.[6] a Conformal Index (COIN) was proposed as a measure of implant quality and dose specification in brachytherapy. COIN is defined as:

The coefficient c_1 is the fraction for the PTV that is enclosed by D_{ref} and is a measure of how accurately the PTV is covered by D_{ref} . The ideal situation is c_1=1:

PTV_{ref} is the part of PTV that is covered by part of the reference dose value, D_{ref}, volume (V_{ref}).
The coefficient c_2 is the fraction of V_{ref} that is covered by PTV. It is also a measure of how much normal tissue outside the PTV is covered by D_{ref}. The ideal situation is c_2=1:
The coefficient c_1 is determined as the DVH value for PTV for the D_{ref} value. The PTV_{ref} is

$$c_1 = \frac{PTV_{ref}}{PTV} \qquad (10)$$

then given by:

$$PTV_{ref} = c_1 \cdot PTV \qquad (12)$$

$$c_2 = \frac{PTV_{ref}}{V_{ref}} \qquad (11)$$

The volume enclosed by the reference dose value D_{ref}, V_{ref}, can be calculated from the dose-volume histogram for the body contour:

$$V_{ref} = DVH_{body} \cdot V_{body} \qquad (13)$$

where DVH_{body} is the DVH value for the body contour for D_{ref}. The coefficient c_2 is then calculated from the above Eqs. 12 and 13 using Eq. 11.

COIN values can also be calculated using the above equations for every other than D_{ref} dose value. The resulting dependence of the conformal index COIN on the dose value, is called COIN distribution. Usually the dose values are normalized to D_{ref} and are given either as fractions or percentage of D_{ref} .
The "ideal" dose distribution (see Fig. 3) is characterized by the following:

- COIN = 1 at D= D_{ref}, which means that the reference dose value isodose 3D envelope is identical with the planning target volume (PTV). This criterion is stronger than to require a variance of the dose values on the surface of PTV equal to 0.
- For D< D_{ref}, an extremely rapid fall-off of the COIN value which corresponds to a rapid fall-off of the dose outside the PTV (normal tissues).
- COIN ≈ 0 for D> D_{ref}, that means that there are negligible volumes with dose values higher than D_{ref}.

According to the "ideal" dose distribution the following objectives for the COIN based optimization, can be defined:

- Maximization of the COIN value at D= D_{ref}
- Minimization of the integral I_1 of the COIN distribution in the interval [0, D_{ref}),
- Minimization of the integral I_3 of the COIN distribution in the interval (c· D_{ref}, ∞],

The three integrals of the COIN distribution I_1, I_2 and I_3 corresponding to the intervals of the dose values [0, D_{ref}), (D_{ref}, c· D_{ref}] and (c· D_{ref}, ∞] are shown in Fig. 4. The coefficient c

describes the proportion of the reference dose that is considered to represent clinically high dose values. Values of c=1.5 have been proposed in the literature[1,7]. Although there is no compelling argument for this we will accept this value for the following discussion. In the case where critical structures have to be considered, the additional objective of minimizing volumes in these structures with dose values higher than a critical value D_{crit} can be defined. Using the differential dose-volume histograms for these structures this can be expressed as:

- Minimization of the integral I_{crit} of the differential dose-volume histogram for the interval $[D_{crit}, \infty]$.

C. Implementation of a multiobjective genetic optimization algorithm

In the present implementation of our multiobjective genetic algorithm a population of strings is formed, each string storing a set of weights for each source dwell position. The weights are initially produced randomly distributed in the interval [0.0, 1.0]. The next generation is populated using a tournament selection or a roulette wheel selection method based on dominance. After a new population is formed, the strings of random selected pairs undergo a crossover operation with a probability P_c and mutation with a probability P_m. P_c and P_m can be selected free, experience although shows that both must be limited in the range 0.7-1.0 and 0.001-0.1 respectively. The size of the population can be also selected but should be larger than 50. Various crossover types can be selected: single point, two point, and arithmetic crossover. For the mutation operation two methods can be selected: a uniform and a non-uniform mutation. Usually chromosomes in genetic algorithms are represented as binary strings. We also used a floating point representation. Several tests have shown[17] a better performance for the floating point representation, especially for problems with a large number of decision variables. For the tournament selection, the tournament population size is a free parameter. Tests have shown that it should be normally 10% of the population size. For much smaller values the genetic algorithm is sensitive to fluctuations, while much larger values can lead to a premature convergence. The tournament size can be used for the modification of the selective pressure. We applied special genetic operators for decision variables with a real value representation as described by Michalewicz[17]. Some of them offer the possibility for a better performance of the genetic algorithms in the late stage of the optimization process.

Uniform mutation

In a binary representation a chromosome string is formed of several elements or bits. It is only a single bit that is flipped. For the floating point representation, if g_k is the k^{th} element of a chromosome selected for mutation, then it is replaced by a random number from the interval [LB,UB] where LB and UB are the lower and upper bounds of the k^{th} element.

Non-uniform mutation

If g_k is the k^{th} element of a chromosome at generation t it will be transformed after a non-uniform mutation to g_k'

$$g_k' = \begin{cases} g_k + ?(t, UB - g_k) & \text{if } r_1 = 0 \\ g_k - ?(t, g_k - LB) & \text{else} \end{cases} \qquad (14)$$

$$?(t, y) = y \cdot (1 - r^{(1-\frac{t}{T})^b}) \qquad (15)$$

where r_1 is a random bit (0 or 1), r is a random number in the range [0,1], T is the maximal generation number and b a parameter controlling the dependency of $\Delta(t,y)$ on the generation number. The function $\Delta(t,y)$ returns a value in the range [0,y] such that the probability of $\Delta(t,y)$ being close to 0 increases as t increases. Initially when t is small the space is searched

uniformly and very locally at later stages. Random digits are produced by the routine irbit1 provided by Numerical Recipes[23].

Arithmetic crossover

If g_i^t and g_j^t are two chromosomes of the population at generation t, then after arithmetic crossover two new chromosomes g_i^{t+1}, g_j^{t+1} at generation t+1 are produced:

$$g_i^{t+1} = a \cdot g_j^t + (1-a) \cdot g_i^t \qquad (16)$$

$$g_j^{t+1} = a \cdot g_i^t + (1-a) \cdot g_j^t$$

α is either a constant (uniform arithmetical crossover), or a variable depending on the generation number (non-uniform arithmetical crossover).

Multiobjective Elitism

If desired a multiobjective elitism is applied at each generation. Members with the best ever result for each objective are stored and additionally one member closest to the ideal optimum. These members are guaranteed to exist during the whole lifetime of the population.

Selecting the Solution from the Pareto Set

After the last generation is processed by the genetic algorithm, members of the population are expected to be close to the Pareto frontier of the set **F**. Members forming a Pareto frontier (based on dominance) are selected. A member of this set is selected which has a minimum Euclidean distance to the ideal optimum (e.g. COIN=1.0 and I_3=0.0). The distance is calculated by normalizing each objective to a maximum value of 1 using the corresponding largest objective value in the population. This member is presented as the solution of the optimization process. Additionally members are selected each with the best result in each objective. A list is produced with the objective values for all the members of the Pareto frontier. Additionally the user can examine the COIN distributions and the dose-volume histogram and isodose contours of every member of the population. Based on this information of the trade-off surface of the various objectives the decision maker can select the best result. In our current implementation each objective has equal priority. The selection methods can be modified if a preference or ranking on the objectives is necessary without using any arbitrary weights describing the ranking as in Yu et al[10].

The Genetic Multiobjective Dose Optimization Algorithm

The pseudo-code for the genetic multiobjective dose optimization algorithm is given in the flow chart of Fig. 5.
The differential and cumulative dose-volume histograms are calculated by sampling the dose distribution of in total 100000-120000 random distributed points inside the PTV, the body and the critical structures. Points generated inside the PTV are not considered if they are in parts of critical structures which are defined inside the PTV (as in the case of prostate and urethra). Points inside a volume are not allowed to be closer than a given distance to the source dwell positions (depending on the outer radius of the catheters used) removing thus high dose values which have no clinical relevance, for example dose points within catheters. Since the major computational part is limited to the calculation of the dose-volume histograms for each member of the population, the random points inside the volumes are produced only once, at the beginning. The distances of these points and of the dose points produced on the surface of the PTV (see later) from each separate source dwell position r_{ij} (more precisely the inverse square distances $1/r_{ij}^2$) are stored for speed maximization in look-up tables. In order to further reduce the calculation time the dose distribution is

calculated assuming a $1/r^2$ dependence and ignoring any spatial anisotropy, namely attenuation and scattering effect. This dosimetric simplification has no measurable influence on the results of the optimization. Because the NSGA and NRGA selection methods require a previous sorting or ranking of the whole population of each generation this is very time consuming. Although all three selection methods NPGA, NSGA and NRGA are provided in our software and can be used, our investigation has shown that the NPGA algorithm results in equivalent solutions with much less computation time. This is because for the NPGA method there is no need for sorting or ranking pre-calculations for each generation.

All calculations presented in our study have been made by using for the mutation probability P_m a value of 0.0065 and for the crossover probability P_c a value of 0.85. Furthermore a uniform mutation option has been selected and a two point crossover has been used. The selection of a two point crossover means that the string representation of a member is cut at two random positions and the two end parts are interchanged. This increases the efficiency of the exploitation[22] . Here we mention that all presented selection methods and genetic operators in this section are implemented in our software and can be selected by the user if needed.

Results presented in this work were produced on a PC with an Intel Pentium II 400 MHz processor with 256 MB RAM. The optimization time depends mainly on the number of possible dwell positions and the population size. For 200 dwell positions and up to 100 generations it can take 4-5 hours. Fig. 6a shows the population average of the COIN Integral I_3 for $D>1.5 \cdot D_{ref}$ versus generation number showing a convergence after 200-300 generations for an optimization of an representative implant with 200 source dwell positions. The convergence is faster for smaller number of source dwell positions. The convergence of the population average of the COIN value at $D = D_{ref}$ is shown in Fig. 6b.

Parallelisation of the calculations should increase the velocity approximately proportional to the number of processors available. An optimization of the sampling points at which the dose values are calculated could increase the speed by a factor of at least 2-3. If points on a grid are used, instead randomly distributed points, then the calculation of the dose distribution with Fourier transforms is expected to increase the speed generally by a factor of 10. Additional software engineering optimization techniques are expected to increase the speed by a factor of 2-3.

Material

Four different cases consisting of a geometrical test implant and three clinical implants (see Table I) were investigated in this study with our Multiobjective Genetic Algorithm using the Offenbach brachytherapy methodology[6]. The geometrical characteristics of these implants are given in Table I. These implants have been selected to cover a large area of our clinical experience and practice in Offenbach with PTV volumes varying from 33cm³ to 496cm³, number of catheters per cm³ in the PTV from 0.02 to 0.55 and number of dwell positions per cm³ PTV from 0.4 to 1.8. With the PROMETHEUS software[24] the implanted catheters were reconstructed. On the surface of the PTV, equidistant dose points were generated with a defined density, depending on the size of the PTV, usually at a distance 0.5-2.0 cm. These points are used for the definition of the mean dose value at the surface of PTV that is initially used as the reference dose D_{ref}. The active dwell positions to be used for the optimization are defined along the catheters and it is ensured that they are inside the PTV at a distance of 0.5-1.0 cm below the PTV surface. The whole reconstruction information is then transferred via network to the PC where optimization using our multiobjective genetic algorithm is carried out. For each member of the population for a given generation and if needed, a renormalization is carried out according to the resulting COIN distribution, so that the maximum COIN value is observed at $D=D_{ref}$ (see also Baltas et al.[6]). This results generally in mean normalized dose values at the surface of PTV different from 1.0. The dose prescription is realized at the D_{ref}, the isodose value resulting in the maximal conformity. Our results are compared with those from the conventional dose optimization algorithms obtained with the PLATO BPS[#] treatment planning system (version 13.5, CT based reconstruction and microSelectron-HDR) as found in our clinical routine. The same patient files with the CT images, the PTV and organ contours created in the PLATO system were used by the PROMETHEUS software. In both cases, with PLATO and PROMETHEUS, the same sampling density for the dose points on the surface of PTV and the same active source dwell positions were selected. For purposes of comparison, the results in terms of dwell position weights obtained with PLATO, were imported in our software (ASCII source loading files) and using these the DVHs for the PTV and the critical structures if any, and the resulting COIN distributions were calculated together with those for our own best solution. The size of the volumes of the PTV, the body and the critical structures must be known with a high degree of accuracy for the calculation of the COIN spectra. For the determination of the geometrical volumes we use a simple Monte Carlo method. A large number of random points (300,000) inside the bounding box of each structure (PTV, body, organs) is produced. The fraction of points inside the structure to the points inside the associated bounding box is equal to the fraction of the structure volume to the bounding box volume. From the known bounding box volume, the volume of the structure is then calculated.

A. Spherical PTV Test Implant

Fig. 7 shows the 3D contours of the spherical PTV implant with the 40,000 randomly distributed points inside the PTV, which are used to calculate the dose-volume histograms and the COIN distributions. This test implant has been generated for a spherical PTV with a radius of 2.5cm with 44 source dwell positions in 34 catheters (see Table I). The source dwell positions are distributed on a surface lying 0.8cm below the PTV surface and keeping inter-source distances of 0.8cm-1.3cm. A source position has then to be entered at the centre of the spherical PTV. For this geometrical distribution of the source dwell positions in the spherical PTV there is a global maximum for the optimization of the dose distribution. If this is concentrated only on the variance of dose values on the PTV surface as is the case for the 'on dose points only' optimization method in the PLATO BPS system where the weight of the

[#] Nucletron B.V., Veendendaal, The Netherlands.

central dwell position is set to one and all others to 0. This is why this implant has been used to prove whether the MOGA algorithm can escape from this trap.

B. Clinical Cases

Breast Implant

A clinical breast implant with a PTV of 115.5cm³ and 10 plastic catheters with 212 dwell positions selected inside the PTV has been used as representative of a middle-sized volume implant. Fig. 8 shows the 3D PTV contours for the breast implant. This implant results in a catheter density of 0.1 catheters per cm³ and a source dwell position density of 1.8 dwells per cm³.

Prostate Implant

A prostate implant carried out with four metallic catheters and a total of 37 source dwell positions has been selected to represent a small volume implant (PTV of 32.9 cm³, see Table I) with the urethra as a critical structure surrounded by the PTV. Fig. 9 shows the 3D contours of the PTV and urethra for the prostate implant.

Rib Implant

A very large volume implant (PTV of 495.9 cm³, see Table I) with the left kidney as a critical structure outside the PTV for a rib metastasis with soft tissue components. A total of 12 plastic catheters have been inserted with a resultant total number of source dwell positions inside the PTV of 172. This corresponds to a catheter density of 0.02 catheters per cm³ and a source dwell position density of 0.4 dwells per cm³. The low density of catheters and source dwell positions can be explained by the difficulty of this anatomical location and by the shape of PTV (see Fig. 10).

Results

The following results for our MOGA method have been obtained using the COIN value maximization, I_3 COIN integral minimization and I_{crit} integral minimization for critical structures. These are the minimum set of objectives that can be used for the optimization of the 3D brachytherapy dose distribution. For reasons of simplicity, instead of maximizing the COIN value our software considers as an objective the minimization of 1-COIN. The MOGA solution is that which is automatically selected by our software from the population of the Pareto frontier after 300 generations (see Fig. 6). It is also noted that the weight results from both systems are normalized to the maximum weight value observed for each system.

A. Spherical PTV Test Implant

The results of the MOGA method together with those using the 'dose points and geometry' optimization method of BPS are shown in Fig. 11. Two objectives are used in the MOGA: maximization of the COIN value at $D = D_{ref}$ and minimization of the COIN integral I_3 at the interval $(1.5 \cdot D_{ref}, \infty]$. On the surface of the PTV 537 dose points have been generated and have be used to define the mean dose on the surface of the PTV. An optimization based only on the minimization of the variance of the dose values on these points ('on dose points only' option), would produce a result giving a weight value of 1.0 for the dwell position 35 at the center of the sphere and keeping all other weights equal to 0, due to the geometrical symmetry of the dwell positions.
Comparison of the COIN distribution for MOGA and that for 'dose points and geometry' (see Fig. 11a) shows that MOGA, with two objectives, produces a more homogenous dose distribution inside the PTV, keeping the same conformity as the conventional method. The COIN value at D_{ref} of 0.86 *versus* 0.85 is shown in Table II. The mean dose value in the PTV is reduced from 1.5±0.5 to 1.4±0.4 and the maximum dose value in the PTV from 76.1 to 4.4 for the conventional and for the MOGA methods respectively, whereas the minimum dose value in the PTV is almost the same (0.8 *versus* 0.6) as seen in Table III. On the other hand, the variation of the dose values on the PTV surface is higher with the MOGA method. This gives a standard deviation of 0.2 *versus* 0.1 as seen in Table II. All dose values are normalized to the D_{ref} and are expressed as proportions of the D_{ref} value as mentioned previously. The reduction of the inhomogeneity with MOGA is clearly visible in the dose volume histograms in Fig. 11b where a significant reduction of dose values higher than $1.5 \cdot D_{ref}$ is shown. This reduction corresponds to a PTV volume of 13.5cm³ (22%).
The weight distributions for both methods are shown in Fig. 11c. The MOGA method gives a 0 weight value at the central dwell position whereas the conventional method gives a value of 1.0.

B. Clinical Cases

Breast Implant

This is an example of a medium-sized implant. We investigated the results obtained with all conventional optimization methods available in PLATO BPS[8]. The genetic algorithm provides a solution with a more homogenous dose distribution inside the PTV than any conventional algorithm (Fig. 12). Even the COIN value at $D = D_{ref}$ is slightly better (Fig. 12a, Table II): 0.88 for MOGA *versus* 0.86 for the clinical applied optimization method 'on dose points and geometry', whereas the variation of the dose on the PTV surface remains almost the same as seen in Table II. A total of 537 dose points on the surface of the PTV were generated and were used to define the mean dose on the surface of the PTV.
Analyzing the differential dose-volume histograms (Fig. 12b) the MOGA method gives a significant reduction of dose values higher than $1.5 \cdot D_{ref}$ (objective I_3 COIN integral) that correspond to PTV volumes of 14cm³ to 22cm³ (12% - 19% of PTV). This is also shown in

Table III where the mean dose value and the maximum dose value in the PTV are significantly reduced using the MOGA method (1.4±0.5 *versus* 1.8±0.8 and 4.9 *versus* 10.3) but where the minimum dose value remains the same.

Figure 13 shows that the weights are mainly distributed among 8-10 dwell positions for the conventional methods, whereas for MOGA they are distributed among 30-40 dwell positions at catheters lying at the periphery (see Fig. 8 and 13c). The weights of the dwell positions of the central catheters 6 and 7 (dwell positions 44 to 83) are small. This explains the greater inhomogeneity resulting from the conventional methods as demonstrated in Figure 12b.

Prostate Implant

This is an example of a small implant with a PTV of only 32.9cm³. We considered the dose optimization in the presence of the urethra as a critical structure enclosed by the PTV. On the surface of the PTV a total of 232 dose points were used. Optimization with the genetic algorithm includes as a third objective the minimization of the dose inside the urethra. This is achieved by performing a minimization of the integral of the differential dose-volume histogram I_{crit} of the urethra above $1.5 \cdot D_{ref}$. This corresponds to a clinically selected critical dose value for urethra of 150% of the reference dose.
The MOGA method and the clinically applied optimization method 'on dose points only' give almost equivalent results for the PTV (see Figure 14 and Tables II and III). Considering the results for the urethra in Table IV, we can summarize the MOGA method results by stating that we have achieved significantly lower mean dose (1.2±0.2 *versus* 1.5±0.3), minimum and maximum dose values (0.6 *versus* 0.7 and 1.6 *versus* 2.4) in the urethra. This is also well demonstrated in Figure 14c where it is seen that a significant reduction has occured of dose values higher than $1.5 \cdot D_{ref}$ (objective I_{crit}), corresponding to the intra-prostate urethra volume of 0.98cm³ (47% of the intra-prostate urethra volume). The DVH for the MOGA method is shifted to lower dose values by a factor of 0.6 of the reference dose value. The reason for this is seen in the distribution of the weights in Figure 14d. Here the MOGA method strongly reduces the weights of the dwell positions of the catheter numbered 3 which is situated near the urethra as seen in Fig. 9.

Rib Implant

This case is an example of an anatomically large volume which is difficult to implant. The left kidney was considered as a critical structure lying adjacent to the PTV. Clinically, the critical dose value was $0.4 \cdot D_{ref}$. A total of 983 equidistant dose points were generated on the surface of the PTV have been used for the analysis of the dose values on the PTV surface.
MOGA method results in a lower COIN value as seen in Figure 15a and Table II, than the conventional methods using the 'dose points and geometry' option (0.69 *versus* 0.78) and a higher variation in the dose values on the PTV surface (0.6 *versus* 0.2). On the other hand there is a significant improvement in the dose value statistics within the PTV. The mean dose values were 1.5±0.9 *versus* 1.7±1.3, the maximum dose values were 17.3 *versus* 29.5 and the minimum dose values were almost the same, 0.4 *versus* 0.3. This is also seen in Figure 15b where there is a significant reduction of dose values higher than $1.5 \cdot D_{ref}$ (objective I_3) that corresponds to a PTV volume of 75.5cm³ (15% of PTV).
The MOGA method results in much improved results compared with conventional methods with regard to the of the left kidney critical structure, a significant reduction of the maximum dose to the kidney as seen in Table IV, 0.6 *versus* 0.8. The mean and the minimum kidney dose values, remain the same. It is also demonstrated in Figure 15c that there is a significant reduction of dose values higher than $0.4 \cdot D_{ref}$ (objective I_{crit}) that corresponds to a kidney volume of 40cm³ (17% of left kidney). The distribution of the weights for both optimization methods are shown in Figure 15d.
For this clinically difficult implant we see that the significant improvement in the dose distribution to the left kidney has been achieved at the expense of some degree of

conformity of the dose distribution for the PTV although the dose distribution within the PTV was more homogeneous than for the conventional method. In clinical practice such a trade-off is often necessary.

Conclusions

A Multiobjective genetic algorithm MOGA was developed for the optimization of dose distributions in brachytherapy. It is based on an *a posteriori* approach, leaving the decision making process to the clinician and medical physicist so that they can choose for an individual patient the optimum trade-off between the various objectives. MOGA provides a flexible and robust search engine which takes into account the maximum available information, and as such is of advantage for decision makers. This is in contrast with previous work[11], where the dose distributions of optimization algorithms were compared with those obtained by manual optimization. We compare the results of our genetic algorithm with the best available conventional optimization algorithms. Other single objective genetic algorithms use only a limited variation of weights, often only 0 or 1, whereas we use weights that can take any value with a accuracy limited only by the arithmetic machine precision. Tests performed with various treatment plans in brachytherapy have shown that MOGA results in solutions superior than that of traditional dose optimization algorithms. Objectives were proposed in terms of the COIN distribution and differential dose-volume histograms, taking into account patient anatomy in the optimization process.

Software engineering optimization and implementation of parallelisation of our software will significantly reduce calculation time. Future work will involve studying more clinical situations in order to reduce optimization times. A further improvement in the performance of the MOGA optimization method can then be achieved by using hybrid versions, namely, those in combination with deterministic searching methods.

The rapid developments in computer technology and the parallel nature of the genetic algorithms will in the near future make MOGA a practical tool for dose optimization purposes in radiotherapy. This is especially valid for an inverse planning software system for clinical interstitial implants using a single stepping source.

LITERATURE

[1]International Commission on Radiation Units and Measurements, ``Dose and Volume Specification for Reporting Interstitial Therapy'', ICRU Report 58, Bethesda, Md: ICRU Publications, 1997.

[2] N. Zamboglou, ``Interstitial brachytherapy possibilities''. In: Zamboglou N., ed., New developments in interstitial remote controlled brachytherapy. Munich: Zuckswerdt; 174-180, 1997.

[3]L. L. Anderson, ``A 'natural' volume-dose histogram for brachytherapy'', Med. Phys. 13, 898-903 (1986).

[4]L. L. Anderson, ``Dose specification and quantification of implant quality'', In: J. F. Williamson, B. R. Thomadsen, R. Nath, eds., Brachytherapy physics, American Medical Physics Publishing Corporation, 343-360, 1995.

[5]Ravinder Nath, Kenneth Roberts, Michelle Ng, Richard Peschel, and Zhe Chen,``Correlation of medical dosimetry quality indicators to the local tumor control in patients with prostate cancer treated with iodine-125 interstitial implants'', Med. Phys. 25, 2293-2307 (1998).

[6]D. Baltas, C. Kolotas, K. Geramani, R. F. Mould, G. Ioannidis, M. Keckidi and N. Zamboglou,``A Conformal Index (COIN) to evaluate implant quality and dose specifications in brachytherapy'', Int. J. Radiation Oncology Biol. Phys, Vol. 40, No. 2, 512-524 (1998).

[7]G. K. Edmundson, ``Geometry based optimization for stepping source implants", in: Brachytherapy HDR and LDR, A. A. Martinez, C. G. Orton and R. F. Mould eds., Nucleotron: Columbia, 184-192, 1990.

[8]R. Van der Larsen, T. P. E. Prins, ``Introduction to HDR brachytherapy optimisation'', In: R. F. Mould, J. J. Batterman, A. A. Martinez and B. L . Speiser eds. Brachytherapy from Radium to Optimization. Veenendaal, The Netherlands: Nucleotron International, pp. 331-351, 1994.

[9]R. Van der Larsen, T. P. E. Prins, ``Comparing the stepping source dosimetry system and the Paris system using volume-dose histograms of breast implants'', In: R. F. Mould, J.J. Batterman, A. A. Martinez and B. L . Speiser eds. Brachytherapy from Radium to Optimization.
Veenendaal, The Netherlands: Nucleotron International, pp. 352-372, 1994.

[10]Y. Yu and M. C. Schell, ``A genetic algorithm for the optimization of prostate implants'', Med. Phys. 23, 2085-2091 (1996).

[11]Guozhen Yang, L. E. Reinstein, S. Pai, and Zhigang Xu, ``A new genetic algorithm technique in optimization of permanent ^{125}I prostate implants.'', Med. Phys. 25, 2308-2315 (1998).

[12]A. Oszycska, ``Multicriteria optimization for engineering design'', John S. Gero, editor, Design Optimization, Academic Press 1985, pp. 193-227.

[13]C. M. Fonseca and P. J. Fleming, ``Multiobjective optimization and multiple constraint handling with evolutionary algorithms I: A unified formulation", Research report 564, Dept. Automatic Control and Systems Eng, University of Sheffield, Sheffield, U.K., Jan. 1995.

[14]C. M. Fonseca, P. J. Fleming, ``An overview of evolutionary algorithms in multiobjective optimization", Evolutionary Computation 3(1), 1-16 (1995).

[15]I. Das and J. Dennis, ``A Closer Look at Drawbacks of Minimizing Weighted Sums of Objectives for Pareto Set Generation in Multicriteria Optimization Problem'', Structural Optimization, Vol. 14, No. 1 (1997).

[16]J. R. Koza, Genetic Programming: On the Programming of Computers by Means of Natural Selection, Massachusetts, MIT Press, 1992.

[17]Z. Michalewicz, Genetic Algorithms + Data Structures =Evolution Programs, Springer Verlag, 1996.

[18]D. E. Goldberg and J.Richardson, ``Genetic Algorithms with Sharing for Multimodal Function Optimization'', J.J. Grefenstette (Editor), Genetic Algorithms and Their Applications: Proceedings of the Second International Conference on Genetic Algorithms, Lawrence Erlbaum Associated, pp. 41-49, 1987.

[19]D. E. Goldberg, Genetic Algorithms in Search, Optimization and Machine Learning, Addison Wesley, Reading, Massachusetts, 1989.

[20]J. Horn and N. Nafpliotis, ``Multiobjective optimization using the niched Pareto genetic Algorithm'', IlliGAL Report No.93005. Illinois Genetic Algorithms Laboratory. University of Illinois at Urbana-Champaign, 1993.

[21]N. Srinivas and K. Deb, ``Multiobjective Optimization Using Nondominated Sorting in Genetic Algorithms'', Evolutionary Computation, 2(3), pp. 221-248 (1994).

[22]International Commission on Radiation Units and Measurements, ``Prescribing, Recording, and Reporting Photon Beam Therapy'', ICRU Report 50, Bethesda, Md: ICRU Publications, 1990.

[23]W. H. Press, S. A. Teukolsky, W.T. Vetterling, B. P. Flannery, Numerical Recipes in C,2nd ed., Cambridge University Press, Cambridge, England, 1992.

[24]A. Tsalpatouros, D. Baltas, C. Kolotas, C. Koutsouris, D. Uzunoglou, N. Zamboglou,``CT based software for 3-D Localisation and Reconstruction in Stepping Source Brachytherapy'', IEEE Trans. Inform. Techni. Biomed. 1:229-242 (1997).

Tables

Implant	PTV (cm^3)	Number of catheters	Catheters per cm^3	Number of dwells positions	Dwell positions per cm^3	Number of dose points
Spherical phantom	61.8	34	0.55	44	0.7	537
Breast	115.5	10	0.09	212	1.8	770
Prostate	32.9	4	0.12	37	1.1	232
Rib	495.9	12	0.02	172	0.4	983

TABLE I. Characteristics of the four implants used in this study.

	COIN		$D_{surf} \pm 1$ S.D.	
Implant	Conventional method	MOGA	Conventional method	MOGA
Spherical phantom	0.85	0.86	0.91 ± 0.06	0.91 ± 0.20
Breast	0.86	0.88	1.00 ± 0.17	0.91 ± 0.19
Prostate	0.67	0.66	0.83 ± 0.19	0.83 ± 0.28
Rib	0.78	0.69	0.91 ± 0.16	1.00 ± 0.60

TABLE II. Results of both conventional and MOGA optimization methods for the four implants for the COIN values at $D=D_{ref}$ and the mean dose values D_{surf} at the surface of the PTV. All dose values are normalized to the D_{ref} and are expressed as proportions of the D_{ref} value. The conventional results for the breast implant are those using the 'on dose points and geometry' option in PLATO BPS.

	D_{volume} ± 1 S.D.		D_{min}		D_{max}	
Implant	Conventional method	MOGA	Conventional method	MOGA	Conventional method	MOGA
Spherical phantom	1.51 ± 0.48	1.36 ± 0.44	0.80	0.61	76.05	4.37
Breast	1.80 ± 0.82	1.44 ± 0.48	0.61	0.55	10.33	4.93
Prostate	1.66 ± 0.97	1.53 ± 0.93	0.38	0.38	9.55	10.50
Rib	1.71 ± 1.25	1.46 ± 0.86	0.27	0.37	29.47	17.31

TABLE III. Results of conventional and MOGA optimization methods for the four implants for the mean dose values D_{volume}, minimum dose values D_{min} and maximum dose values D_{max} within the PTV. All dose values are normalized to the D_{ref} and are expressed as proportions of the D_{ref} value. The conventional results for the breast implant are those using the 'on dose points and geometry' option in PLATO BPS.

		D_{volume} ± 1 S.D.		D_{min}		D_{max}	
Implant	Critical structure	Conventional method	MOGA	Conventional method	MOGA	Conventional method	MOGA
Prostate	Urethra	1.47 ± 0.33	1.17 ± 0.23	0.74	0.64	2.42	1.64
Rib	Kidney	0.33 ± 0.12	0.29 ± 0.10	0.16	0.15	0.81	0.60

TABLE IV. Results of conventional and MOGA optimization methods for the four implants for the mean dose values D_{volume}, minimum dose values D_{min} and maximum dose values D_{max} within the critical structures. All dose values are normalized to the D_{ref} and are expressed as proportions of the D_{ref} value.

Figure Legends

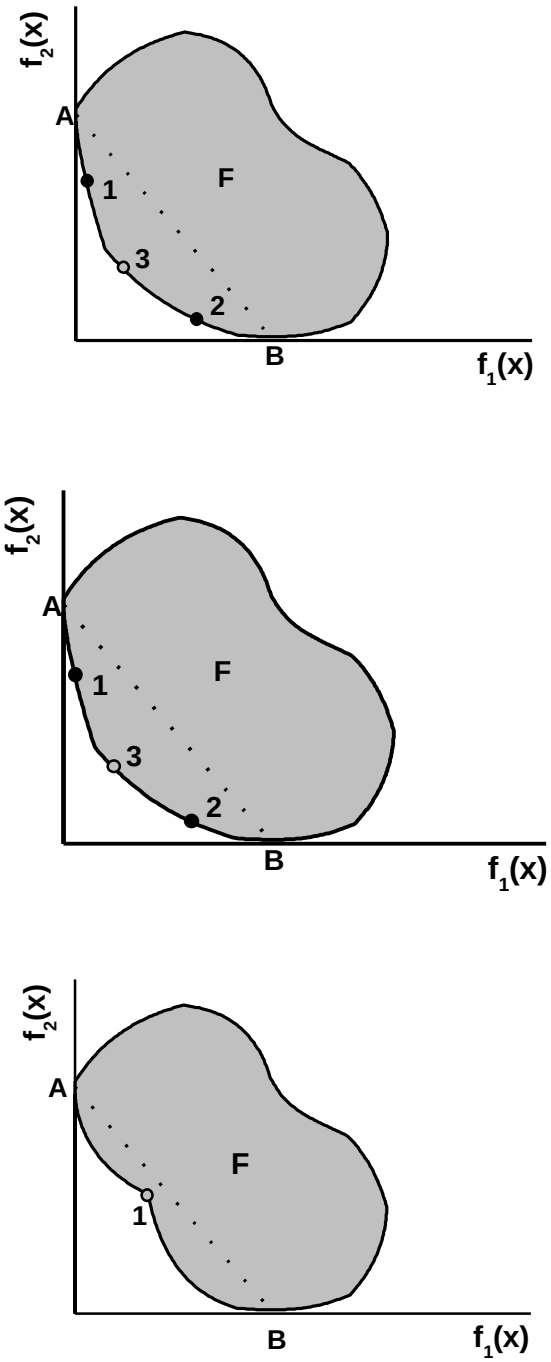

Figure 1. Bi-loss map for the objectives f_1 and f_2. (a) A typical case (b) The case of non-uniform sampling of points on the Pareto frontier (c) The case of a non-convex Pareto frontier.

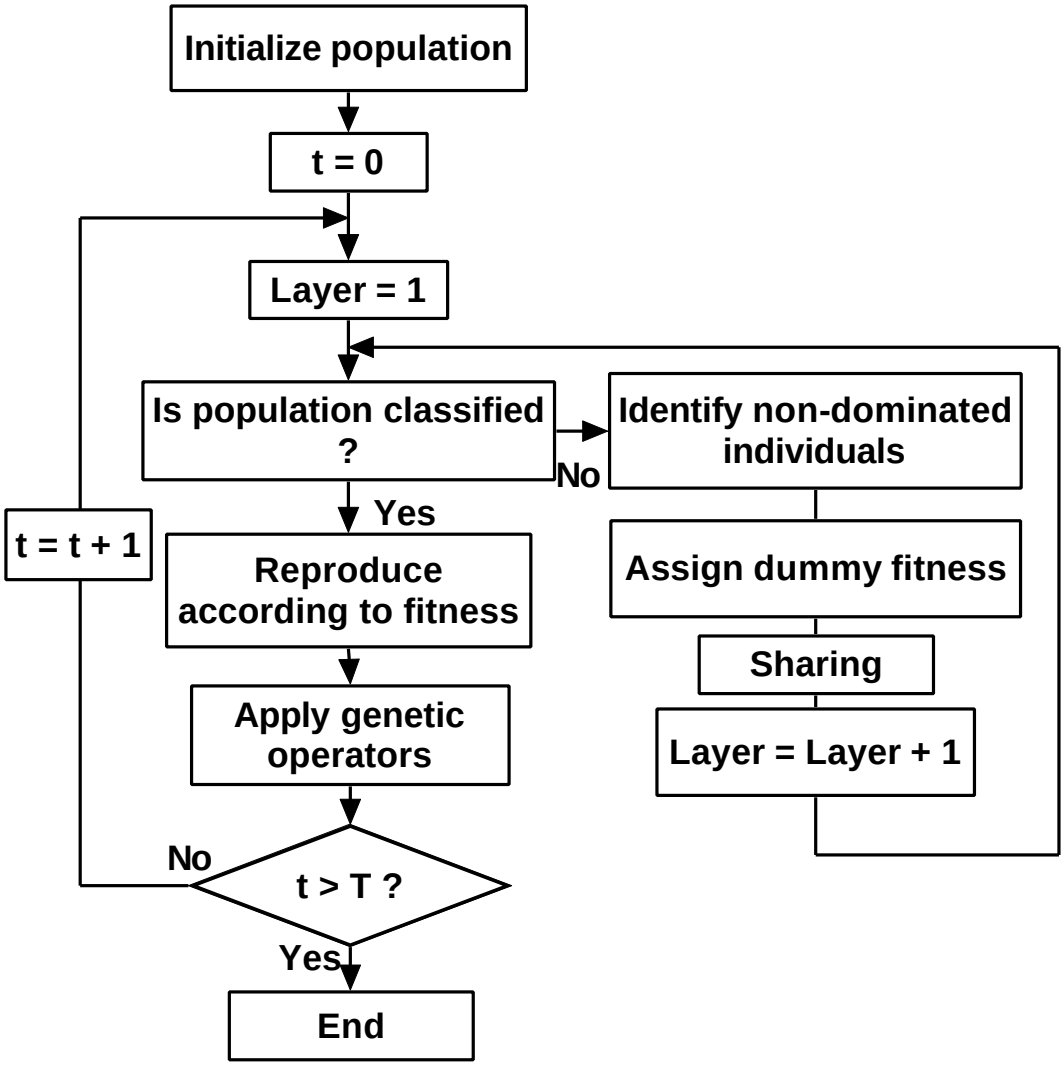

Figure 2. Flow chart of the NSGA algorithm.

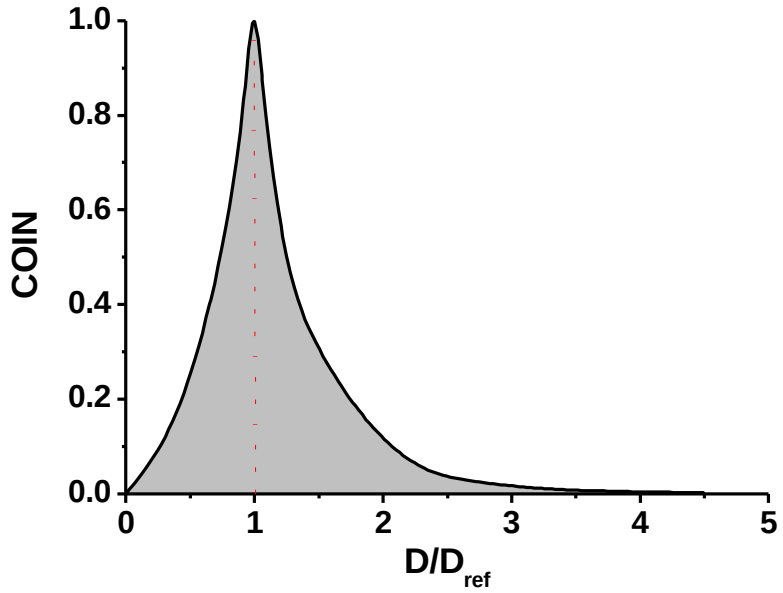

Figure 3. An ideal COIN distribution. The dose values are normalized to the D_{ref} reference dose and are expressed as fractions of D_{ref}.

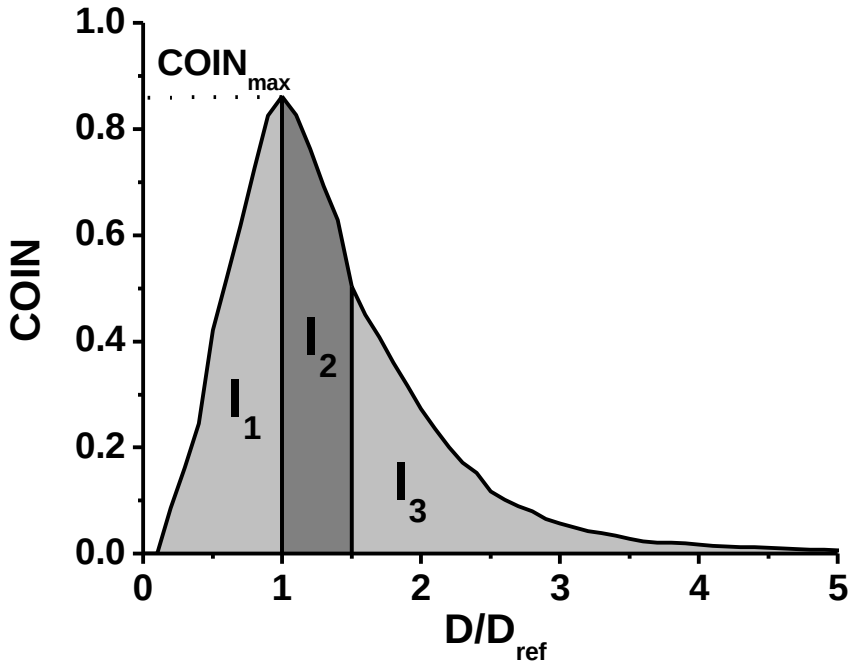

Figure 4. Definition of the COIN integrals I_1, I_2 and I_3 of the COIN distribution.

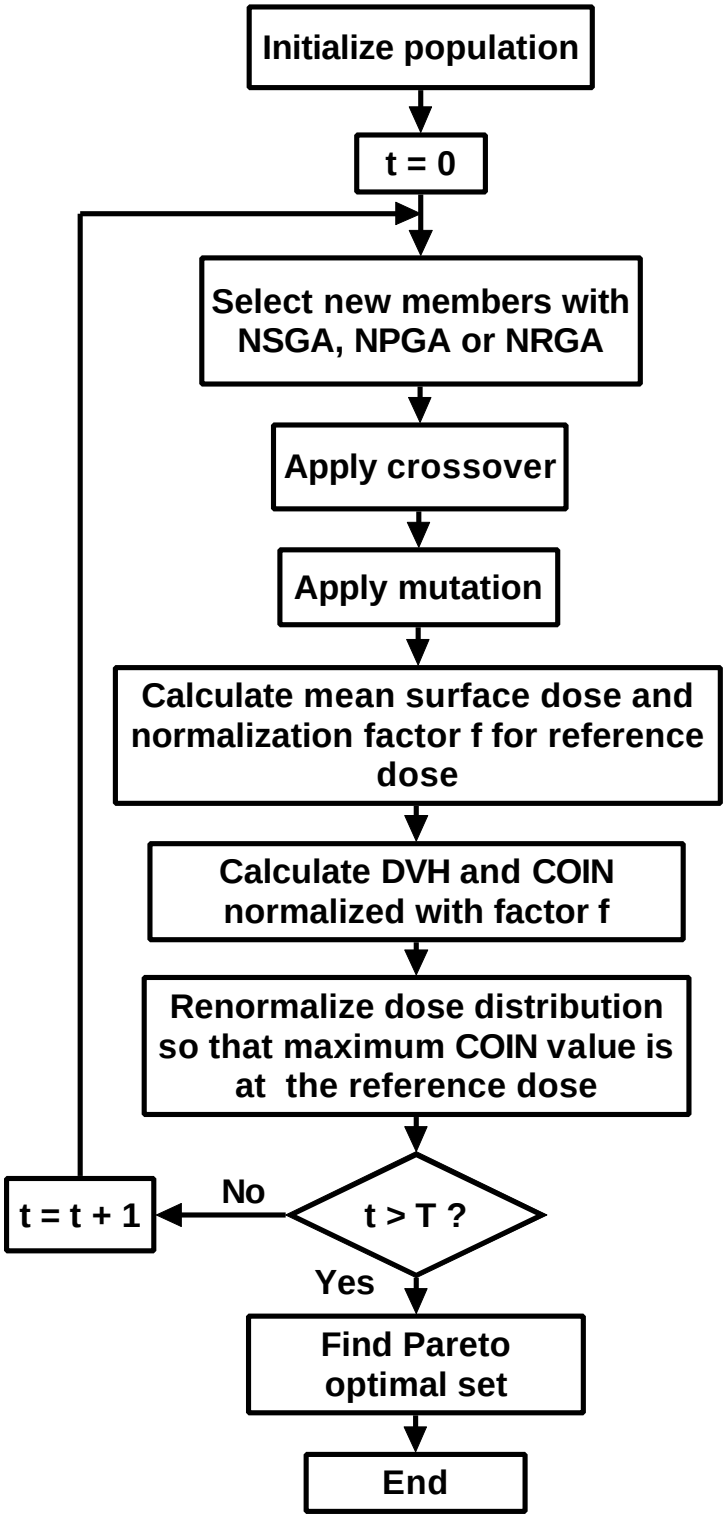

Figure 5. Flow chart of the multiobjective genetic dose optimization algorithm.

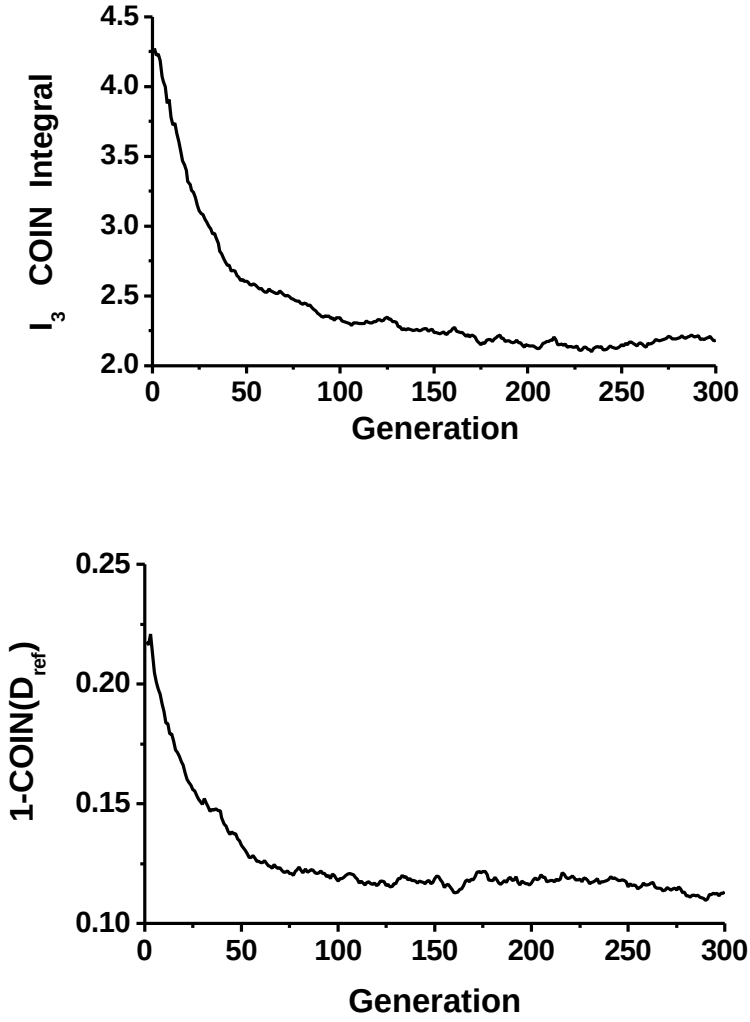

Figure 6. Typical convergence of the population averaged indexes *versus* the generation number for our MOGA implementation. (a) For the COIN integral I_3 (b) For (1-COIN(D_{ref})) values.

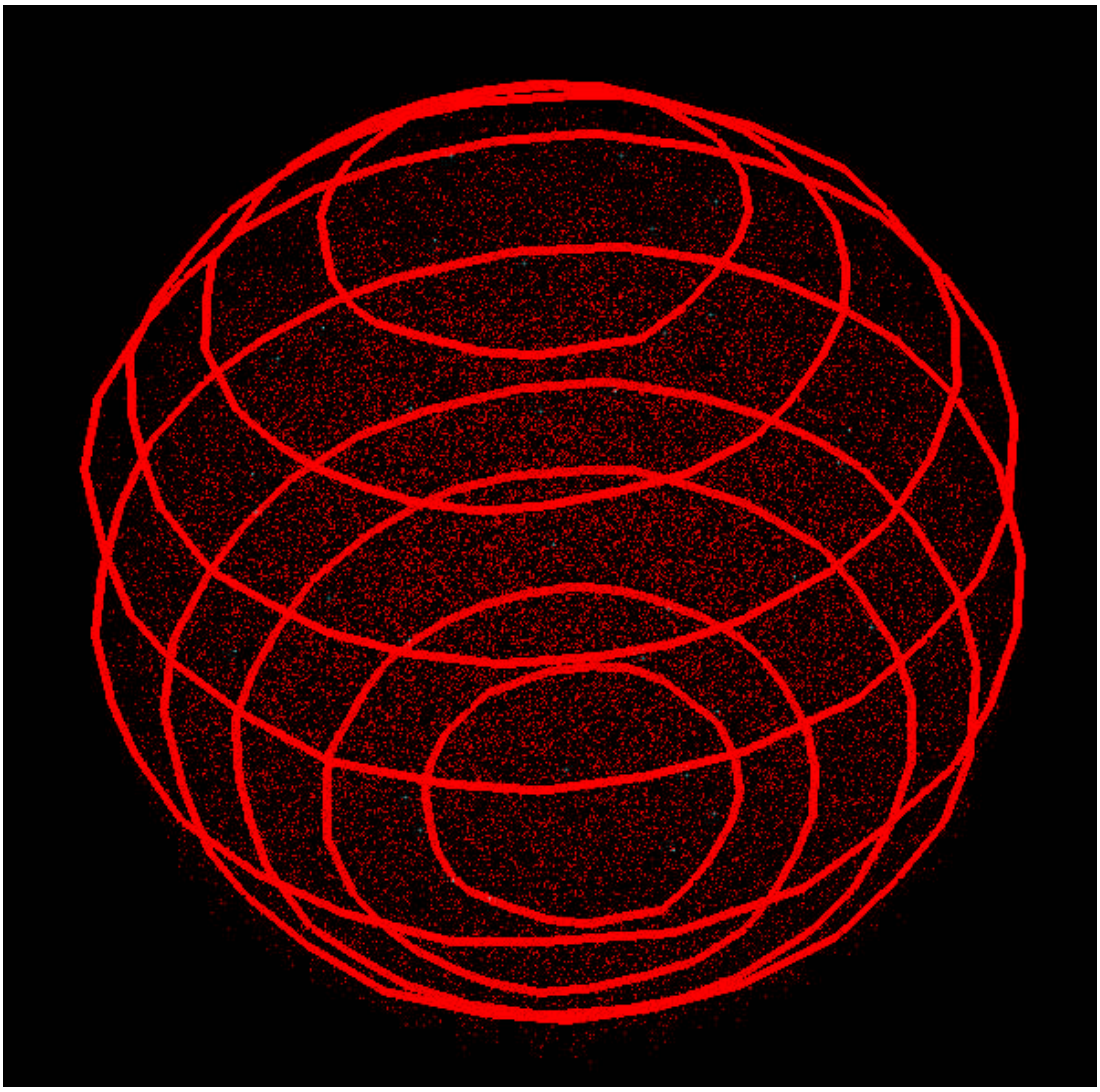

Figure 7. Contours of a spherical PTV test implant with 40,000 random points generated within the PTV which are used to calculate the DVH and COIN distribution for the optimization procedure.

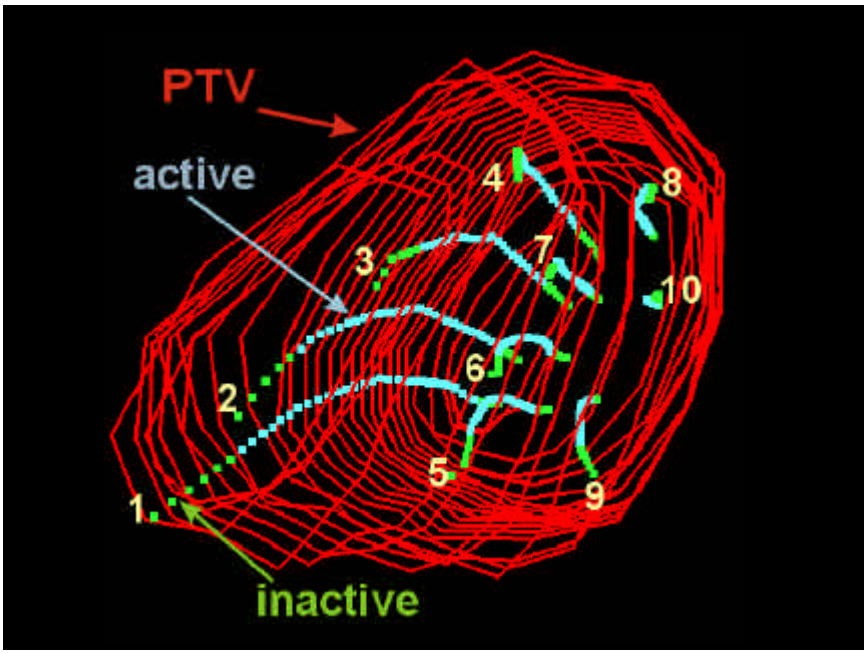

Figure 8. 3D contours of the PTV with the selected active dwell positions (blue) for the 10 catheters for the breast implant. The dwell positions that are not selected for inclusion in the optimization (inactive) are shown in green. The numbers of the catheters are shown at the catheter connector end.

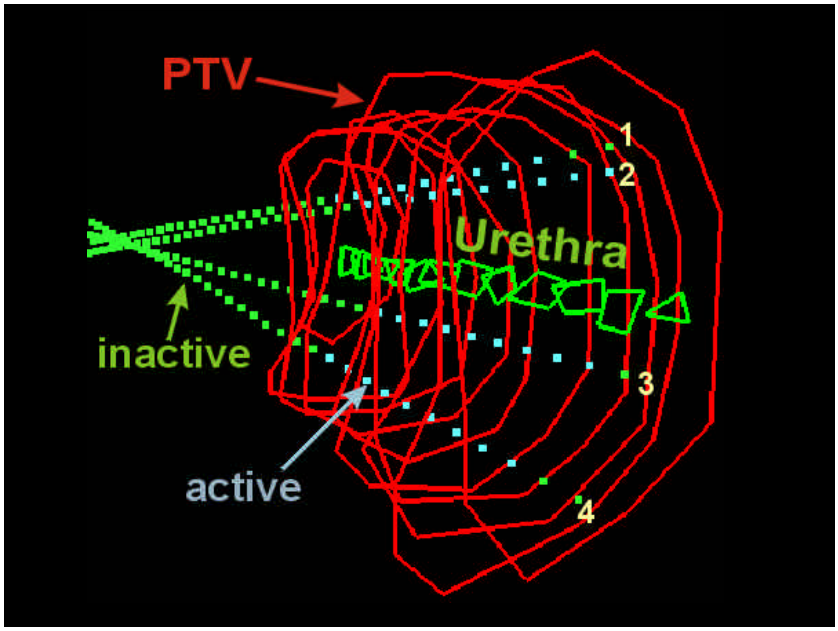

Figure 9. 3D contours of the prostate implant including the PTV, and the urethra as a critical structure inside the PTV. The four catheters and the active (blue) and inactive (green) source dwell positions are also shown. The numbers of the catheters are shown at the catheter tip.

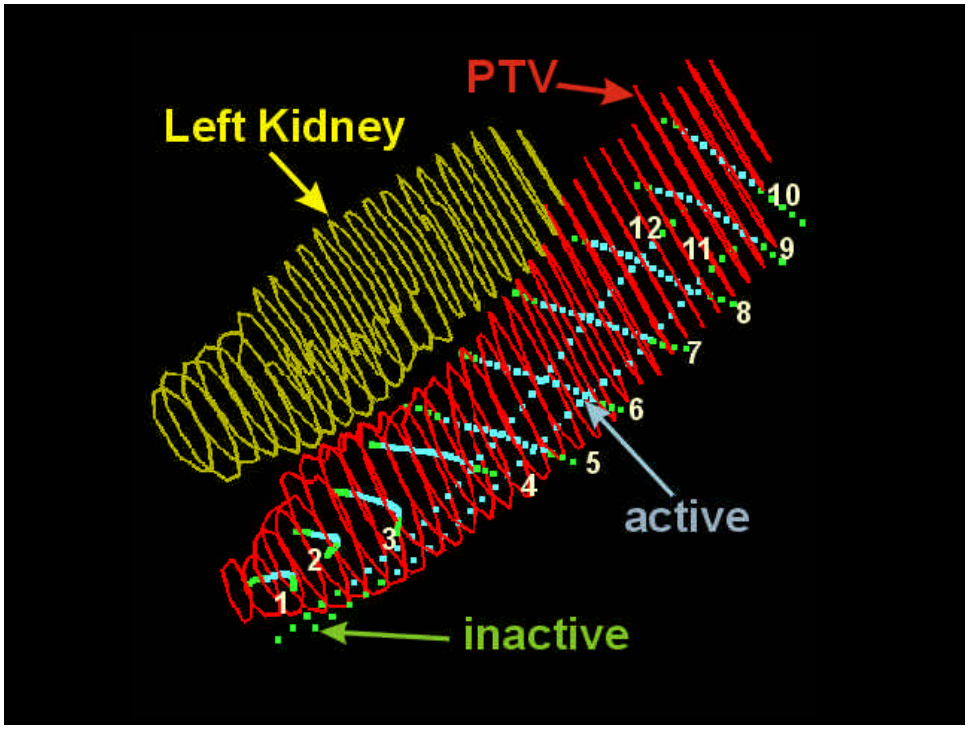

Figure 10. 3D contours for the rib implant including the PTV, and the left kidney as a critical structure outside the PTV. The 12 catheters and the active (blue) and inactive (green) source dwell positions are also shown. The numbers of the catheters are shown at the catheter tip.

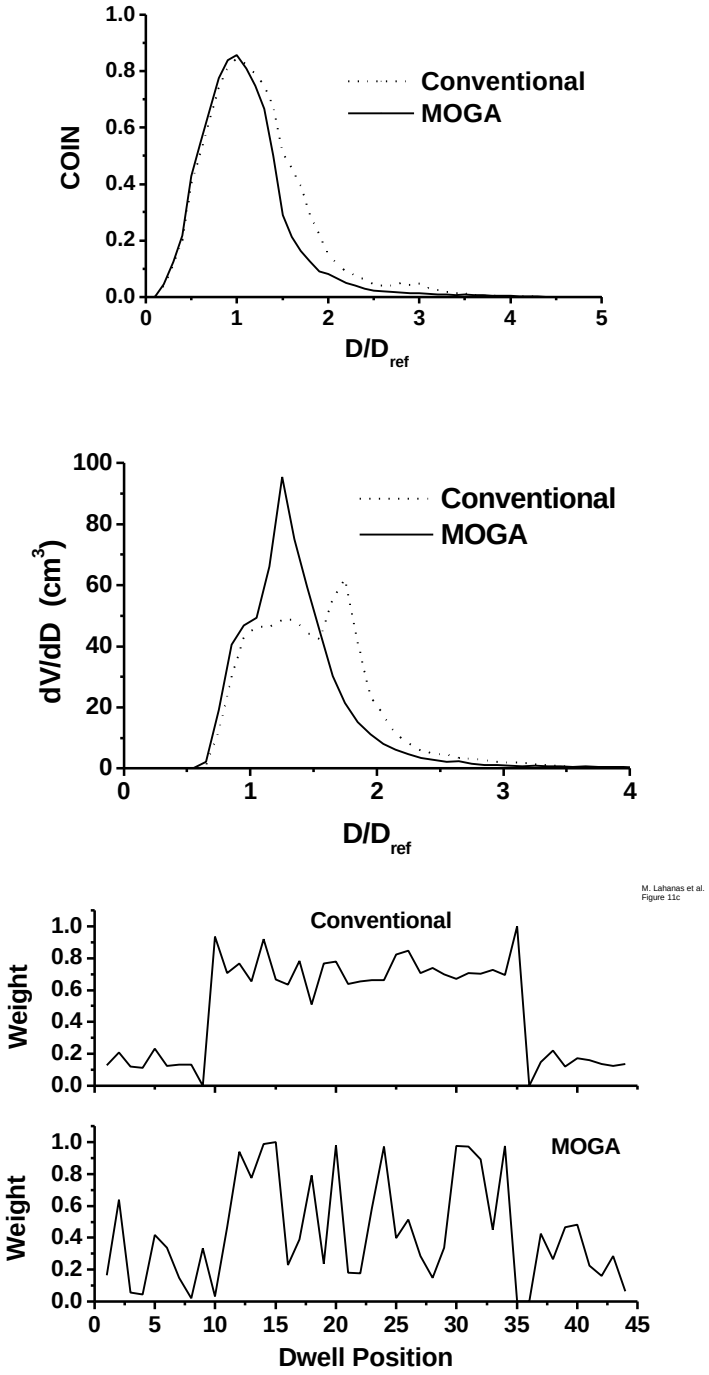

Figure 11. Comparison of the results of our multiobjective optimization method with that of the conventional method using the 'on dose points and geometry' optimization of the PLATO BPS system for the spherical PTV test implant. (a) COIN distributions (b) Differential dose-volume histograms for PTV. (c) Distribution of weights for the 44 active dwell positions. The dwell position numbered with 35 is that positioned at the center of the spherical PTV.

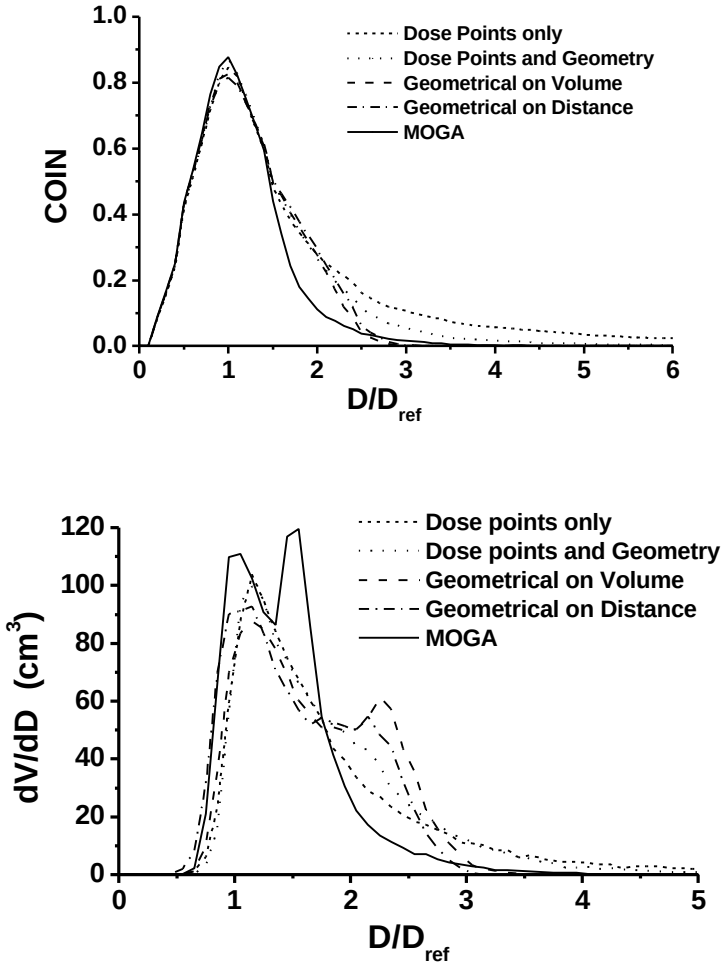

Figure 12. Comparison of the results of our multiobjective optimization method with those of the conventional methods for the breast implant of Fig. 8. All available conventional optimization methods in the PLATO BPS software are included. The clinical treatment was carried out with an optimization using dose points and geometry. (a) COIN distributions (b) Differential dose-volume histograms for the PTV.

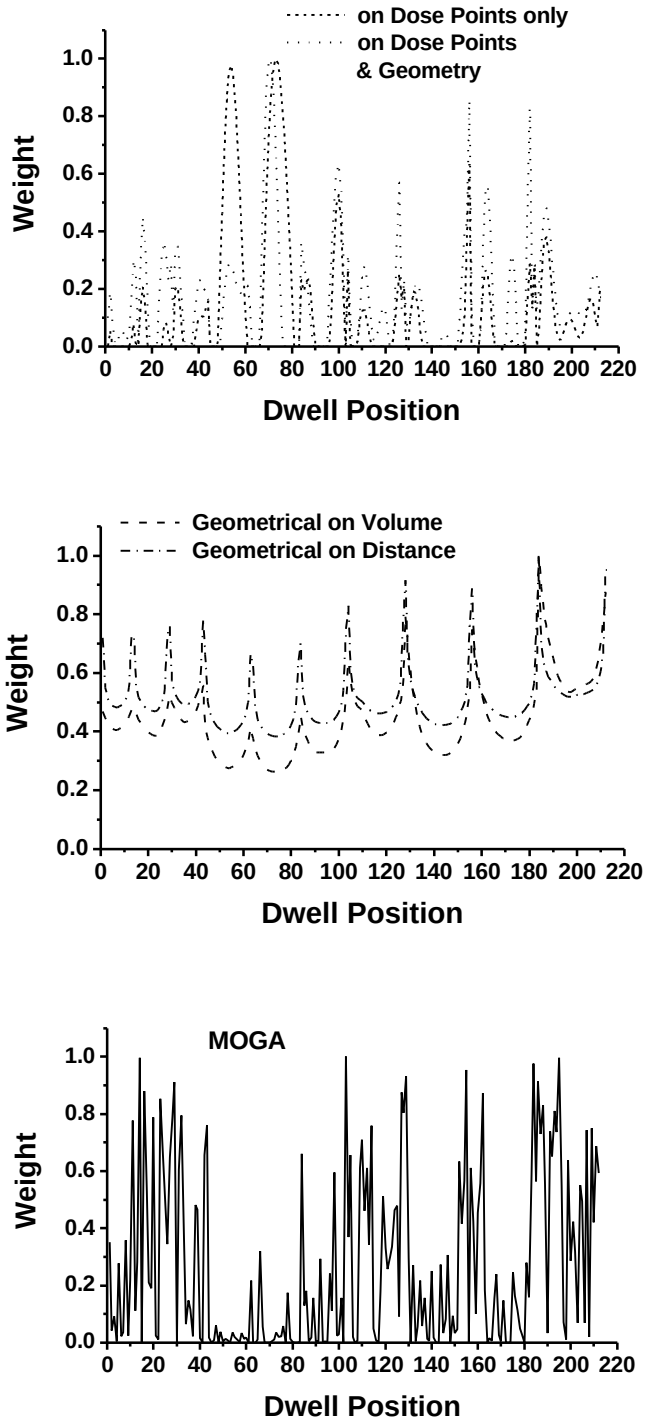

Figure 13. Comparison of the weights of the 212 active dwell positions for the 10 catheters of the breast implant. (a) Dose point optimization (b) Geometrical optimization (c) MOGA methods.

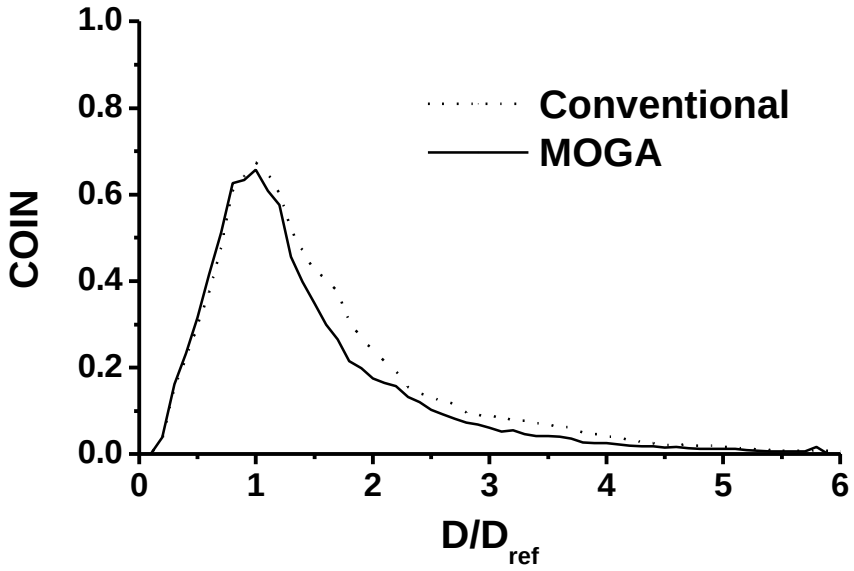
1.0
0.8
0.6
0.4
0.2
0.0
COIN
0
1
2
3
4
5
6
D/D ref
Conventional
MOGA

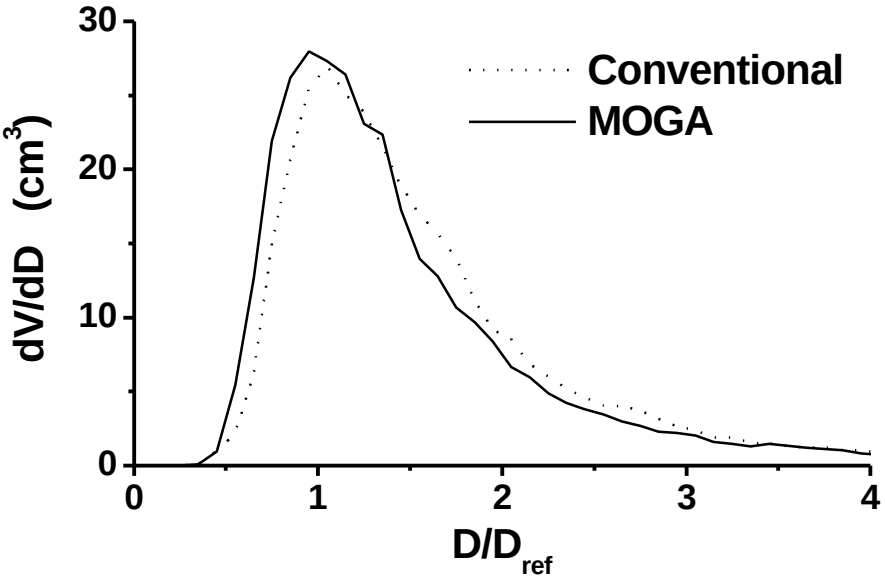
30
20
10
0
dV/dD (cm3)
0
1
2
3
4
D/D ref
Conventional
MOGA

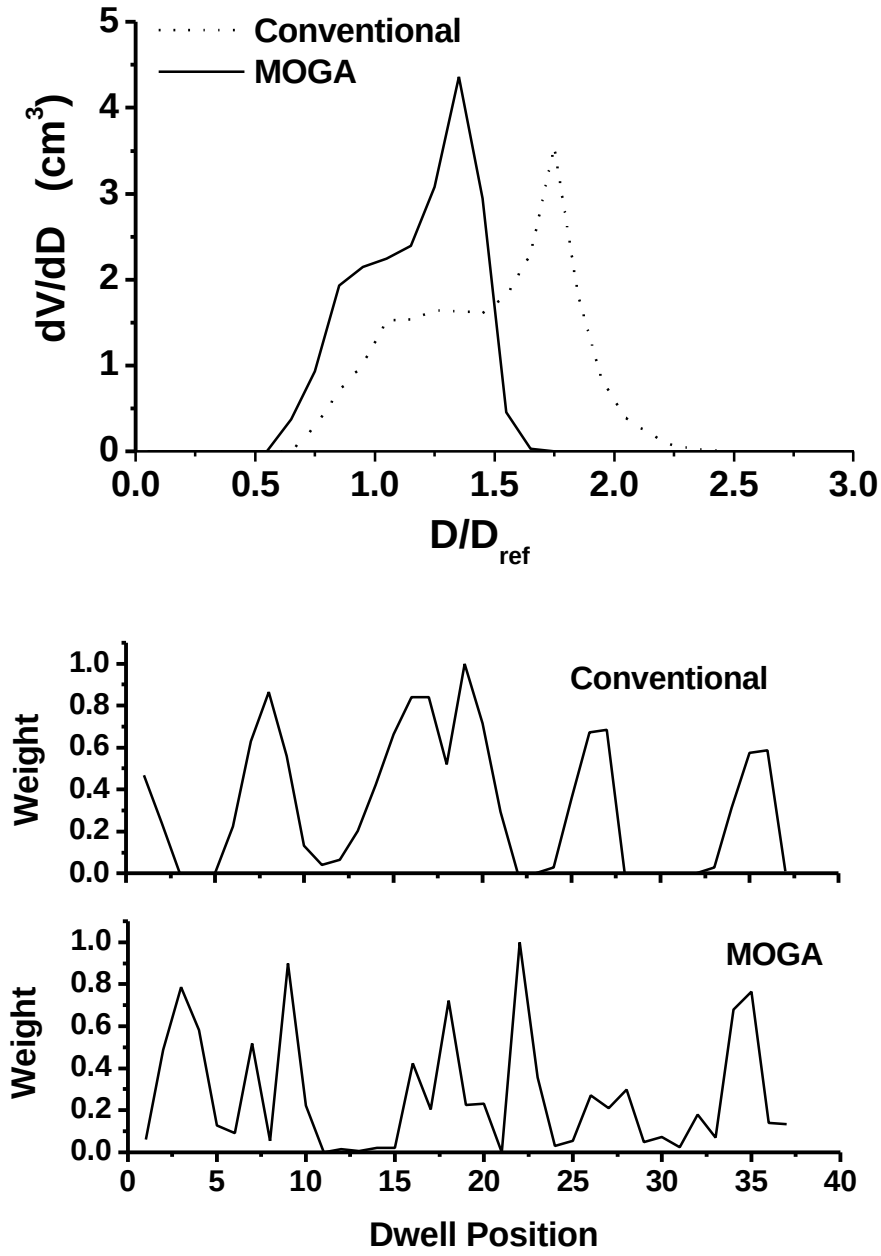

Figure 14. Comparison of the results of our multiobjective optimization method with that of the conventional method using the 'on dose points only' optimization option of the PLATO BPS system for the prostate implant. (a) COIN distributions (b) Differential dose-volume histograms for the PTV (c) Differential dose-volume histograms for the urethra (d) Distribution of weights for the 37 dwell positions.

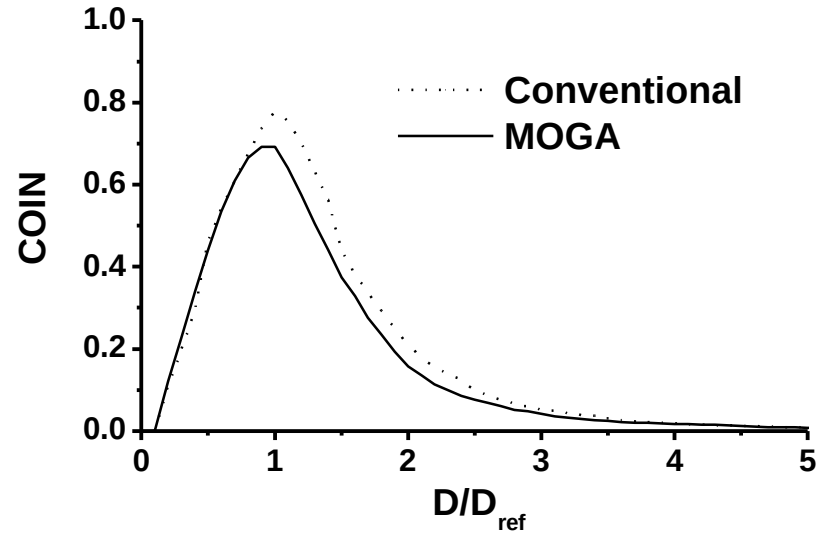
1.0
0.8
0.6
0.4
0.2
0.0
COIN
0
1
2
3
4
5
D/D ref
Conventional
MOGA

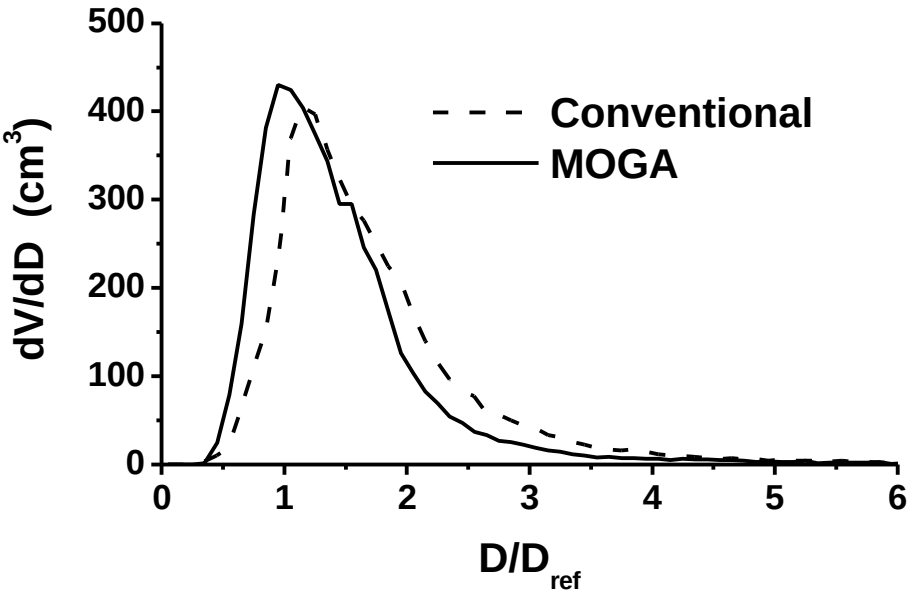
500
400
300
200
100
0
dV/dD (cm3)
0
1
2
3
4
5
6
D/D ref
Conventional
MOGA

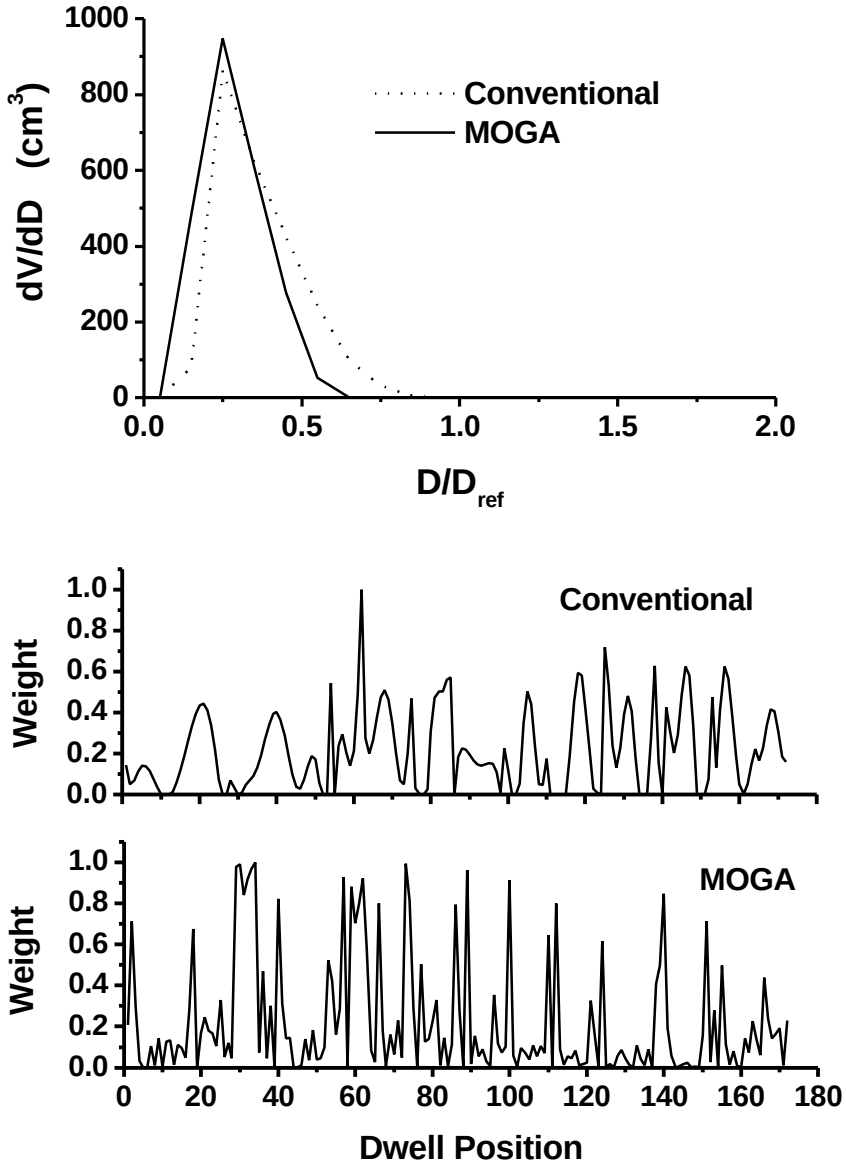

Figure 15. Comparison of the results of our multiobjective optimization method with those of the conventional method using the 'on dose points only' and geometry optimization option of the PLATO BPS system for the rib implant. (a) COIN distributions (b) Differential dose-volume histograms for the PTV (c) Differential dose-volume histograms for the left kidney and (d) Distribution of weights for the 172 dwell positions.